Inorganic Chemistry

Article

Synthesis and Structural Characterization of Nonanuclear Lanthanide Complexes

Gang Xu, Zhe-Ming Wang,* Zheng He, Zhi LU, Chun-Sheng Liao, and Chun-Hua Yan*

State Key Laboratory of Rare Earth Materials Chemistry and Applications, PKU-HKU Joint Laboratory on Rare Earth Materials and Bioinorganic Chemistry, College of Chemistry, Peking University, Beijing 100871, China

A series of nonanuclear lanthanide oxo–hydroxo complexes of the general formula $[Ln_9(\mu_4\text{-}O)_2(\mu_3\text{-}OH)_8(\mu\text{-}BA)_8\text{-}(BA)_8]^-[HN(CH_2CH_3)_3]^+\cdot(CH_3OH)_2(CHCl_3)$ (BA = benzoylacetone; Ln = Sm, **1**; Eu, **2**; Gd, **3**; Dy, **4**; Er, **5**) were prepared by the reaction of hydrous lanthanide trichlorides with benzoylacetone in the presence of triethylamine in methanol and recrystallized from chloroform/methanol (1:10) at room temperature. These five compounds are isomorphous. Crystal data for **1**: cubic, $Pn\bar{3}n$; $T = 180$ K; $a = 33.8652(4)$ Å; $V = 38838.4(8)$ Å^3; $Z = 6$; $D_{calcd} = 1.125$ g cm^{-3}; R1 = 3.37%. Crystal data for **2**: cubic, $Pn\bar{3}n$; $T = 180$ K; $a = 33.8252(8)$ Å; $V = 38700.9(16)$ Å^3; $Z = 6$; $D_{calcd} = 1.133$ g cm^{-3}; R1 = 4.97%. Crystal data for **3**: cubic, $Pn\bar{3}n$; $T = 180$ K; $a = 33.7061(6)$ Å; $V = 38293.5(12)$ Å^3; $Z = 6$; $D_{calcd} = 1.157$ g cm^{-3}; R1 = 5.13%. Crystal data for **4**: cubic, $Pn\bar{3}n$; $T = 180$ K; $a = 33.5900(7)$ Å; $V = 37899.2(14)$ Å^3; $Z = 6$; $D_{calcd} = 1.182$ g cm^{-3}; R1 = 4.03%. Crystal data for **5**: cubic, $Pn\bar{3}n$; $T = 180$ K; $a = 33.5054(8)$ Å; $V = 37613.6(16)$ Å^3; $Z = 6$; $D_{calcd} = 1.202$ g cm^{-3}; R1 = 4.86%. The core of the anionic cluster comprises two vertex-sharing square-pyramidal $[Ln_5(\mu_4\text{-}O)(\mu_3\text{-}OH)_4]^{9+}$ units. The compounds were characterized by elemental analysis, IR, fast atom bombardment mass spectra, thermogravimetry, and differential scanning calorimetry. The thermal analysis indicated that the nonanuclear species were stable up to 150 °C. Luminescence spectra of **2** and magnetic properties of **1**–**5** were also studied.

Introduction

In recent years, self-assembly of nanoscale high-nuclearity metal clusters via methods of coordination chemistry has attracted increasing interest,[1] because these supermolecules exhibit novel structural characteristics[2] as well as important applications in both biology and materials chemistry, especially as potential precursors applied in magnetic, optical, electronic, and catalytic processes for their size-dependent physical properties.[3] To obtain these high-nuclearity clusters, a common synthetic strategy is to control the hydrolysis of metal ions in the presence of appropriate chelating ligands.[4] Many classes of ligands are adequate to the task, including polyketonates, polyamines, polyols, carboxylates, pyridonate, and alkoxides.[5–10] Hydrophilic groups, such as oxo and hydroxo, bridge the metal ions to make up a cluster core, whereas the hydrophobic groups take up positions in the periphery, preventing the core from further aggregation and thus forming a finite-sized polynuclear complex.

* Authors to whom correspondence should be addressed. C.-H. Yan: Tel and Fax, +86-10-62754179; E-mail, chyan@chem.pku.edu.cn.
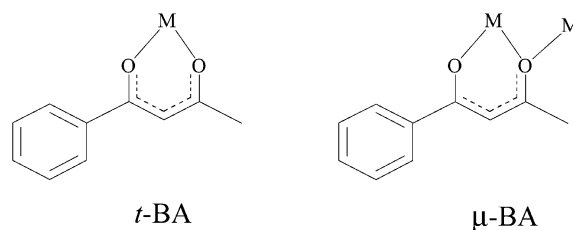
(1) (a) Takeda, N.; Umemoto, K.; Yamaguchi, K.; Fujita, M. *Nature (London)* **1999**, *398*, 794. (b) Olenyuk, B.; Whiteford, J. A.; Fechtenkötter, A.; Stang, P. J. *Nature (London)* **1999**, *398*, 796. (c) Fujita, M. *Chem. Soc. Rev.* **1998**, *27*, 417.
(2) (a) Winpenny, R. E. P. *Chem. Soc. Rev.* **1998**, *27*, 447. (b) Caulder, D. L.; Raymond, K. N. *J. Chem. Soc., Dalton Trans.* **1999**, 1185. (c) Müller, A.; Kögerler, P. *Coord. Chem. Rev.* **1999**, *182*, 3.
(3) (a) Lauffer, R. B. *Chem. Rev.* **1987**, *87*, 901. (b) Sessoli, R.; Gatteschi, D.; Caneschi, A.; Novak, M. A. *Nature (London)* **1993**, *365*, 141. (c) Gatteschi, D.; Caneschi, A.; Sessoli, R.; Cornia, A. *Chem. Soc. Rev.* **1996**, *25*, 101. (d) Pope, M. T.; Muller, A. *Angew. Chem., Int. Ed. Engl.* **1991**, *30*, 215.

(4) Abbati, G. L.; Cornia, A.; Fabretti, A. C.; Caneschi, A.; Gatteschi, D. *Inorg. Chem.* **1998**, *37*, 3759 and references therein.
(5) (a) Caneschi, A.; Cornia, A.; Fabretti, A. C.; Gatteschi, D. *Angew. Chem., Int. Ed.* **1999**, *38*, 1295. (b) Abbati, G. L.; Cornia, A.; Fabretti, A. C.; Malavasi, W.; Schenetti, L.; Caneschi, A.; Gatteschi, D. *Inorg. Chem.* **1997**, *36*, 6443.
(6) Bhula, R.; Weatherburn, D. C. *Angew. Chem., Int. Ed. Engl.* **1991**, *30*, 688.
(7) Cavalluzzo, M.; Chen, Q.; Zubieta, J. *J. Chem. Soc., Chem. Commun.* **1993**, 131.
(8) Steunou, N.; Bonhomme, C.; Sanchez, C.; Vaissermann, J.; Hubert-Pfalzgraf, L. G. *Inorg. Chem.* **1998**, *37*, 901.
(9) (a) Parsons, S.; Winpenny, R. E. P. *Acc. Chem. Res.* **1997**, *30*, 89. (b) Goldberg, D. P.; Caneschi, A.; Delfs, C. D.; Sessoli, R.; Lippard, S. J. *J. Am. Chem. Soc.* **1995**, *117*, 5789.
(10) (a) Mehrotra, R. C.; Singh, A.; Sogani, S. *Chem. Soc. Rev.* **1994**, *23*, 215. (b) Caulton, K. G.; Hubert-Pfalzgraf, L. G. *Chem. Rev.* **1990**, *90*, 969.

Polynuclear lanthanide complexes are receiving much attention due to their distinguished applications. Great efforts have been focused on the europium(III) nanoclusters to construct luminescent nanodevices.[11] Similar interest in gadolinium(III) nanoclusters with tunable electron relaxation behavior can be conceived for magnetic resonance imaging applications.[12] As prominent precursors in sol−gel processes, lanthanide oxo−alkoxide complexes have been studied intensively,[10b,13] whereas reports on polynuclear oxo−hydroxo lanthanide clusters are rather limited. Hexanuclear complexes containing a $[Ln_6(\mu_6\text{-}O)(\mu_3\text{-}OH)_8]^{8+}$ core were synthesized via the direct hydrolysis of lanthanide nitrates and perchlorates.[14] Hubert-Pfalzgraf et al. reported the synthesis of a nonanuclear $[Na(EtOH)_6][Y_9O_2(OH)_8(AAA)_{16}]$ in the presence of β-diketonate allyl acetoacetate ligand under an inert atmosphere.[15] However, in contrast to the well-established cluster chemistry of transition metals,[16] the analogous chemistry of lanthanide is still undeveloped. Limited by current synthetic ability, the synthesis of poly-nuclear lanthanide complexes can hardly be controlled and is usually performed by random self-organization.[17] A systematical work by Zheng et al. was to assemble poly-nuclear lanthanide−hydroxo complexes, containing the cu-bane-like $[Ln_4(\mu_3\text{-}OH)_4]^{8+}$ cluster as a building block, with α-amino acids as the supporting ligands under near physi-ological pH conditions.[18]

In the present case, we found an easy and systematic access to the nonanuclear lanthanide oxo−hydroxo clusters by a partial hydrolysis of the trace water in a methanol reaction mixture in air. To achieve this synthetic goal, we focused on the β-diketonate ligand, benzoylacetone (HBA), which featured different coordination modes (Scheme 1). Although the reaction of lanthanide salts with HBA had already been explored and usually produced mononuclear complexes,[19] we succeeded in fabricating a series of nanoscale nonanuclear lanthanide oxo−hydroxo clusters $[Ln_9(\mu_4\text{-}O)_2(\mu_3\text{-}OH)_8(\mu\text{-}BA)_8(BA)_8]^-[HN(CH_2CH_3)_3]^+\cdot(CH_3OH)_2(CHCl_3)$ (BA = benzoylacetone; Ln = Sm, **1**; Eu, **2**; Gd, **3**; Dy, **4**; Er, **5**), whose structures and unique features are described here.

(11) (a) Parker, D.; Williams, J. A. G. *J. Chem. Soc., Dalton Trans*. **1996**, 3613. (b) de Sá, G. F.; Malta, O. L.; Donegá, C. D.; Simas, A. M.; Longo, R. L.; Santa-Cruz, P. A.; de Silva, E. F. *Coord. Chem. Rev.* **2000**, *196*, 165.

(12) (a) Caravan, P.; Ellison, J. J.; McMurry, T. J.; Lauffer, R. B. *Chem. Rev.* **1999**, *99*, 2293. (b) Li, W. H.; Fraser, S. E.; Meade, T. J. *J. Am. Chem. Soc.* **1999**, *121*, 1413.

(13) (a) Hubert-Pfalzgraf, L. G. *New J. Chem.* **1995**, *19*, 727. (b) Evans, W. J.; Sollberger, M. S. *J. Am. Chem. Soc.* **1986**, *108*, 6095.

(14) (a) Wang, R. Y.; Carducci, M. D.; Zheng, Z. P. *Inorg. Chem.* **2000**, *39*, 1836. (b) Zhang, D. S.; Ma, B. Q.; Jin, T. Z.; Gao, S.; Yan, C. H.; Mak, T. C. W. *New J. Chem.* **2000**, *24*, 61.

(15) Hubert-Pfalzgraf, L. G.; Miele-Pajot, N.; Papiernik, R.; Vaissermann, J. *J. Chem. Soc., Dalton Trans.* **1999**, 4127.

(16) For novel examples, see: (a) Watton, S. P.; Fuhrmann, P.; Pence, L. E.; Caneschi, A.; Cornia, A.; Abbati, G. L.; Lippard, S. J. *Angew. Chem., Int. Ed. Engl.* **1997**, *36*, 2774. (b) Pohl, I. A. M.; Westin, L. G.; Kritikos, M. *Chem. Eur. J.* **2001**, *7*, 3438. (c) Dearden, A. L.; Parsons, S.; Winpenny, R. E. P. *Angew. Chem., Int. Ed.* **2001**, *40*, 151. (d) Xu, Z. Q.; Thompson, L. K.; Miller, D. O. *Chem. Commun.* **2001**, 1170.

(17) Anwander, R. *Angew. Chem., Int. Ed.* **1998**, *37*, 599 and references therein.

(18) Representative work: Zheng, Z. P. *Chem. Commun.* **2001**, 2521 and references therein.

Scheme 1. Two Coordination Modes of Ligand BA

t-BA μ-BA

Experimental Section

Chemicals and Measurements. Lanthanide(III) chlorides were obtained by neutralizing corresponding oxides (Liyang Founder Rare Earth Ltd. Co.; at least 99.99% purity) with concentrated hydrochloric acid, followed by evaporation to near dryness. Other reagents were commercial and were used as received.

Elemental analysis of C, H, and N was performed with a Carlo Erba 1102 elemental analyzer. IR spectra were recorded on a Nicolet Magna 750 FTIR spectrometer in the range 600−4000 cm^{-1} against the neat samples and in the range 50−650 cm^{-1} against the samples mulled in Nujol. Fast atom bombardment mass spectra (FAB MS) (with a thioxo−glycerol matrix) were obtained using a ZAB-HS mass spectrometer. The thermal stability was investigated by thermogravimetry (TG) and differential scanning calorimetry (DSC) with a thermal analyzer (DuPont 2100) in N$_2$ at a heating rate of 2 °C/min, using α-Al$_2$O$_3$ as a reference. The luminescence and excitation spectra were recorded using a Hitachi F-4500 spectro-fluorometer with solid samples sealed in a glass tube. Variable-temperature magnetization characterizations of complexes were performed by using an Oxford MagLab 2000 system in the temperature range 2−300 K. Diamagnetic corrections were esti-mated from Pascal's constants.

Preparation of Compounds. LnCl$_3$·6H$_2$O (Ln = Sm, Eu, Gd, Dy, Er; 1.00 mmol) and benzoylacetone (HBA) (1.78 mmol) were dissolved in ca. 15 mL of methanol. Triethylamine (3.75 mmol) was added dropwise to the above methanol solution, and the mixture was stirred at room temperature for 24 h. Light yellow (for Sm, Eu, Gd, and Dy) or pink (for Er) precipitates were collected by filtration, washed with methanol, and dried in a vacuum (yield: ca. 70%). The product was then dissolved in a mixture of CHCl$_3$/CH$_3$OH (1:10 v/v). The mixture was then filtered, and the filtrate was allowed to stand at room temperature. Cubic-shaped crystals, suitable for X-ray analysis, were harvested after 10 days.

$[Sm_9(\mu_4\text{-}O)_2(\mu_3\text{-}OH)_8(\mu\text{-}BA)_8(BA)_8]^-[HN(CH_2CH_3)_3]^+\cdot(CH_3OH)_2\cdot(CHCl_3)$. Anal. Found: C, 46.26; H, 4.11; N, <0.3. Calcd for C$_{169}$H$_{177}$Cl$_3$NO$_{44}$Sm$_9$: C, 46.28; H, 4.08; N, 0.32. FTIR (cm^{-1}): 3346m, 1599s, 1570s, 1518s, 1486m, 1451m, 1379s, 1306w, 1280m, 999w, 961w, 761w, 716m, 690w. Far-IR (Nujol mull, cm^{-1}): 600w, 558m, 517m, 403sh, 372m, 319m, 190m. Positive ion FAB MS: m/z 102 [HN(CH$_2$CH$_3$)$_3$]$^+$. μ_{eff}^{250K} = 3.8 μ_B, calcd 4.7 μ_B (RT).

$[Eu_9(\mu_4\text{-}O)_2(\mu_3\text{-}OH)_8(\mu\text{-}BA)_8(BA)_8]^-[HN(CH_2CH_3)_3]^+\cdot(CH_3OH)_2\cdot(CHCl_3)$. Anal. Found: C, 45.92; H, 3.76; N, 0.33. Calcd for C$_{169}$H$_{177}$Cl$_3$NO$_{44}$Eu$_9$: C, 46.12; H, 4.06; N, 0.32. FTIR (cm^{-1}): 3347m, 1599s, 1570s, 1518s, 1486m, 1450m, 1375s, 1308w, 1280m, 1000w, 963w, 757w, 715m, 690w. Far-IR (Nujol mull, cm^{-1}): 600w, 561m, 549m, 402sh, 376m, 318m, 175m. Positive ion FAB MS: m/z 102 [HN(CH$_2$CH$_3$)$_3$]$^+$. μ_{eff}^{250K} = 8.3 μ_B, calcd 10.4 μ_B (RT).

$[Gd_9(\mu_4\text{-}O)_2(\mu_3\text{-}OH)_8(\mu\text{-}BA)_8(BA)_8]^-[HN(CH_2CH_3)_3]^+\cdot(CH_3OH)_2\cdot(CHCl_3)$. Anal. Found: C, 45.38; H, 3.60; N, <0.3.

Table 1. Crystallographic Data of **1−5**

	1	**2**	**3**	**4**	**5**
formula	$C_{169}H_{177}Cl_3NO_{44}Sm_9$	$C_{169}H_{177}Cl_3NO_{44}Eu_9$	$C_{169}H_{177}Cl_3NO_{44}Gd_9$	$C_{169}H_{177}Cl_3NO_{44}Dy_9$	$C_{169}H_{177}Cl_3NO_{44}Er_9$
fw	4385.62	4400.11	4447.72	4494.97	4537.81
μ(Mo Kα), Å	0.71073	0.71073	0.71073	0.71073	0.71073
T, K	180	180	180	180	180
space group	$Pn\bar{3}n$	$Pn\bar{3}n$	$Pn\bar{3}n$	$Pn\bar{3}n$	$Pn\bar{3}n$
a, Å	33.8652(4)	33.8252(8)	33.7061(6)	33.5900(7)	33.5054(8)
V, Å^3	38838.4(8)	38700.9(16)	38293.5(12)	37899.2(14)	37613.6(16)
Z	6	6	6	6	6
D_{calcd}, g cm^{-3}	1.125	1.133	1.157	1.182	1.202
μ, mm^{-1}	2.088	2.235	2.385	2.709	3.060
R1, %^{a}	3.37	4.97	5.13	4.03	4.86
wR2, %^{b}	9.13	11.78	12.93	9.88	11.22

^{a} R1 = $\Sigma(||F_o| - |F_c||)/\Sigma F_o$. ^{b} wR2 = $[\Sigma(|F_o|^2 - |F_c|^2)^2/\Sigma(F_o)^2]^{1/2}$.

Calcd for $C_{169}H_{177}Cl_3NO_{44}Gd_9$: C, 45.63; H, 4.02; N, 0.31. FTIR (cm^{-1}): 3568w, 3354m, 1598s, 1570s, 1521s, 1486m, 1452m, 1384vs, 1305w, 1280m, 999w, 962w, 771w, 714m, 690w. Far-IR (Nujol mull, cm^{-1}): 600w, 561m, 553sh, 519m, 403sh, 382m, 320m, 171m. Positive ion FAB MS: m/z 102 [HN(CH$_2$CH$_3$)$_3$]$^+$. μ_{eff}^{300K} = 23.6 μ_B, calcd 23.8 μ_B (RT).

[Dy$_9$(μ_4-O)$_2$(μ_3-OH)$_8$(μ-BA)$_8$(BA)$_8$]$^-$[HN(CH$_2$CH$_3$)$_3$]$^+$· (CH$_3$OH)$_2$·(CHCl$_3$). Anal. Found: C, 44.99; H, 3.83; N, <0.3. Calcd for $C_{169}H_{177}Cl_3NO_{44}Dy_9$: C, 45.15; H, 3.98; N, 0.31. FTIR (cm^{-1}): 3576w, 3358m, 1597s, 1570s, 1513s, 1486m, 1451m, 1379s, 1306w, 1281m, 999w, 963w, 761w, 713m, 689w. Far-IR (Nujol mull, cm^{-1}): 601w, 563m, 552sh, 410sh, 391m, 320m, 172m. Positive ion FAB MS: m/z 102 [HN(CH$_2$CH$_3$)$_3$]$^+$. μ_{eff}^{300K} = 31.6 μ_B, calcd 31.9 μ_B (RT).

[Er$_9$(μ_4-O)$_2$(μ_3-OH)$_8$(μ-BA)$_8$(BA)$_8$]$^-$[HN(CH$_2$CH$_3$)$_3$]$^+$· (CH$_3$OH)$_2$·(CHCl$_3$). Anal. Found: C, 44.76; H, 3.88; N, <0.3. Calcd for $C_{169}H_{177}Cl_3NO_{44}Er_9$: C, 44.72; H, 3.94; N, 0.31. FTIR (cm^{-1}): 3345m, 1599s, 1570s, 1516s, 1486m, 1454m, 1386vs, 1306w, 1282m, 999m, 963w, 761w, 713m, 689w. Far-IR (Nujol mull, cm^{-1}): 601w, 565m, 552sh, 522m, 413sh, 398m, 322m, 175m. Positive ion FAB MS: m/z 102 [HN(CH$_2$CH$_3$)$_3$]$^+$. μ_{eff}^{300K} = 28.3 μ_B, calcd 28.8 μ_B (RT).

X-ray Structure Determination. Intensity data for the five compounds were collected at 180 K on a Nonius KappaCCD diffractometer with graphite-monochromated Mo Kα radiation (λ = 0.71073 Å). Cell parameters were obtained by the global refinement of the positions of all collected reflections. Intensities were corrected for Lorentz and polarization effects and empirical absorption. The structures were solved by direct methods, and refined by full-matrix least squares on F^2 using the SHELX-97 package.[20] All non-H atoms of the nonananuclear anion were refined anisotropically. Locations of H atoms of OH groups were justified by difference Fourier synthesis. H atoms were added geometrically and refined using the riding model. The solvent molecules and the [HN(CH$_2$CH$_3$)$_3$]$^+$ cation could not be revealed by the X-ray analysis, and they were treated as C atoms positioned from the difference Fourier map, with large isotropic thermal factors, in the structure refinement. These atoms are not close to the well-defined anion within 3.4 Å. Thus the solvent molecules and the [HN(CH$_2$-CH$_3$)$_3$]$^+$ cation are severely disordered in the lattice. Even the X-ray data collected at 120 K cannot resolve them. Details of crystallographic data are summarized in Table 1.

(19) (a) Il'inskii, A. L.; Porai-Koshits, M. A.; Aslanov, L. A.; Lazarev, P. I. *Zh. Strukt. Khim.* **1972**, *13*, 277. (b) Butman, L. A.; Aslanov, L. A.; Porai-Koshits, M. A. *Zh. Strukt. Khim.* **1970**, *11*, 46.
(20) Sheldrick, G. M. *SHELX-97*, PC Version; University of Göttingen: Göttingen, Germany, 1997.

Results and Discussion

Synthesis. Generally, the examples of well-characterized finite-sized lanthanide clusters are limited and the syntheses are hard to reproduce. Recent reports of Anwander[17] and Zheng[18] suggest that the hydrolysis of the lanthanide ions supported by suitable ligands may be used as a general approach to form lanthanide clusters. In this investigation, we sought polynuclear lanthanide oxo−hydroxo complexes via the hydrolysis of lanthanide chlorides in alcohol systems in the presence of β-diketone HBA.

The syntheses of **1−5** were accomplished by mixing hydrous lanthanide chlorides with a stoichiometric amount of HBA (Ln:HBA = 9:16) in methanol and subsequently adding a quantity of triethylamine dropwise. The choice of methanol in this study was based empirically on the consideration of slowing down the hydrolysis rate of lanthanide ions. Usually, 24 h was needed to obtain a sufficient precipitation. When triethylamine was first added to the methanol mixture, it preferentially captured the proton from HBA to form [HN(CH$_2$CH$_3$)$_3$]$^+$. Therefore, the ligand BA was ready to chelate and/or bridge the lanthanide ions. As the amount of triethylamine exceeded that of the HBA, the small quantity of crystal water of lanthanide chlorides began to hydrolyze to produce oxo and hydroxo, which could bridge the lanthanide ions and make up a cluster core, while the hydrophobic groups of BA took up positions in the periphery. Consequentially, a nonanuclear lanthanide oxo−hydroxo cluster was obtained as a result of the interplay of kinetics and thermodynamics. These compounds were insoluble in water and extremely soluble in CH$_2$Cl$_2$, CHCl$_3$, ClCH$_2$CH$_2$-Cl, CH$_3$CN, and DMF, while they had poor solubility in alcohols, making the purification of products easy by washing with methanol. Block crystals could be recrystallized from chloroform/methanol and were stable in the presence of the mother liquid. Under the above conditions, we were able to synthesize **1−5** many times. Moreover, the crystals could also be obtained by recrystallizing from CHCl$_3$/CH$_3$OH, CH$_2$-Cl$_2$/CH$_3$OH, ClCH$_2$CH$_2$Cl/CH$_3$OH, or CHCl$_3$/CH$_3$CH(OH)-CH$_3$ or even from CH$_3$CN. Compared with the previous reports, the synthesis route presented here provides an easy way to obtain lanthanide complexes with high nuclearity and high purity.

Crystal Structure. Single-crystal X-ray diffraction analysis revealed that compounds **1−5** were isomorphous. They
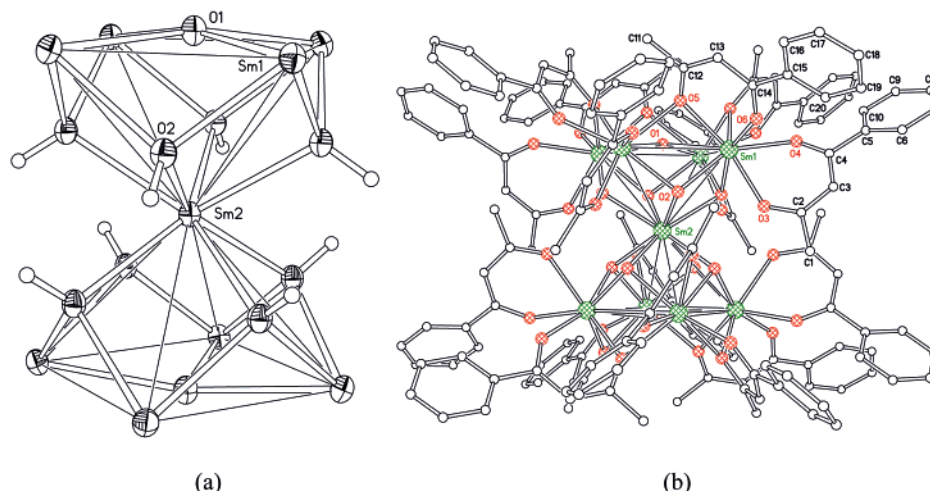
Figure 1. The structure of the nonanuclear anion for **1** with atomic labeling scheme. H atoms are omitted for clarity. (a) The hourglass-like [Ln$_9$(μ_4-O)$_2$-(μ_3-OH)$_8$] core. (b) The whole anion.

are actually ionic species composed of a nanoscaled nonanuclear [Ln$_9$(μ_4-O)$_2$(μ_3-OH)$_8$(μ-BA)$_8$(t-BA)$_8$]$^-$ anion with a counterion of protonated triethylamine ([HN(CH$_2$CH$_3$)$_3$]$^+$) and several solvent molecules. The structure of the anion is shown in Figure 1. The large anion has a nonanuclear [Ln$_9$-(μ_4-O)$_2$(μ_3-OH)$_8$] core and 16 peripheral BA ligands. In the core (Figure 1a), the metal skeleton can be regarded as two square-based pyramidal pentanuclear units assembled via the apical metal (Ln2). As the two square-pyramids are twisted at 45° to each other, the anion is of crystallographic D_{4d} symmetry. Each triangular face of the square pyramids is capped by one μ_3-OH group, so that the central Ln2 ion is surrounded by eight μ_3-OH groups and displays a square-antiprism geometry and also shows a crystallographic D_{4d} symmetry. The distance of the μ_3-OH to the triangular metal face is ca. 1.0 Å. Four Ln1 metal ions in each square base are planar and are linked by one μ_4-O, which is slightly above the basal face. The shift of the μ_4-O [0.253(6)−0.275(8) Å for **1**−**5**] above the Ln$_4$ basal plane is significantly shorter than that observed in the tetradecanuclear [Ln$_{14}$(μ_4-OH)$_2$(μ_3-OH)$_{16}$(o-O$_2$NC$_6$H$_4$O)$_{24}$ (Ln = Er, Yb)]^{21} [0.52 Å], whereas the in-planar μ_4-oxo was observed for [Y$_9$(μ_4-O)$_2$(μ_3-OH)$_8$-(AAA)$_{16}$],^{15} [M$_4$L$_2$(NO$_3$)$_4$(MeOH)$_2$(μ_4-O)] [M = Gd, Tb; L = 1,3-bis(2-hydroxy-3-methoxy-benzylamino)propan-2-ol],^{22} and [Er$_8$(μ_4-O)(μ_3-OH)$_{12}$(thd)$_{12}$] (Hthd = 2,2,6,6-tetramethylheptane-3,5-dione).^{23} The Ln$_9$ core is surrounded by 16 peripheral BA ligands (Figure 1b), which are divided into two classes, eight terminal chelate (t-BA) and eight bridging chelate (μ-BA), according to the coordination behavior of the ligand (Scheme 1). Each Ln1 ion, at the corner of the square bases, is chelated by one t-BA, and further coordinated by two μ-BAs, which link the metal ion with two neighbor metal ions at the corners. Thus Ln1 is coordinated by eight oxygen atoms, two (O3, O4) from the t-BA, three (O5, O6, O5#1) from two μ-BAs, two (O2, O2#1) of μ_3-OHs, and

Table 2. Selected Bond Lengths (Å) of **1**−**5**

bond	**1**	**2**	**3**	**4**	**5**
Ln1−Ln1	3.6971(3)	3.6725(4)	3.6462(4)	3.6038(3)	3.5657(4)
Ln1−Ln2	3.7761(2)	3.7590(3)	3.7430(3)	3.7025(2)	3.6726(3)
Ln1−O(BA)	2.342(3)−	2.333(4)−	2.323(4)−	2.296(4)−	2.284(4)−
	2.476(3)	2.459(4)	2.456(4)	2.423(3)	2.411(4)
Ln1−O2	2.358(3)	2.337(3)	2.332(4)	2.309(3)	2.284(4)
	2.371(3)	2.358(3)	2.340(4)	2.309(3)	2.290(4)
Ln1−O1	2.6264(6)	2.6090(8)	2.5921(9)	2.5626(8)	2.5363(9)
Ln2−O2	2.464(3)	2.455(3)	2.444(4)	2.415(3)	2.396(4)
Ln2−O1	2.978(6)	2.969(7)	2.981(8)	2.957(7)	2.945(8)

one μ_4-O, in a distorted bicapped (O1 and O4) trigonal prism with a coordination environment of C_{2v} symmetry. It is worth noting that the distances of Ln−O and Ln−Ln decrease gradually as Ln varies from Sm to Er, in accordance with the decrease on the radii of the lanthanide ions (Table 2). The Ln−O distances follow the order Ln1−O(t-BA) ≈ Ln1−μ_3-OH < Ln2−μ_3-OH ≈ Ln1−O(μ-BA) < Ln1−μ_4-O < Ln2−μ_4-O, while the Ln⋯Ln distances simply follow Ln1⋯Ln1 < Ln1⋯Ln2. For **2** (Ln = Eu), the Eu−O bond lengths ranging from 2.333(4)−2.6090(8) Å are comparable with those Eu−O distances, 2.321(12)−2.691(10) Å, in the [Eu$_5$-(μ_4-OH)(μ_3-OH)$_4$(DBM)$_{10}$] (DBM = dibenzoylmethide),^{24} whereas the Ln1⋯Ln1 distance is longer and the Ln1⋯Ln2 distance is shorter than those in the latter pentanuclear Eu$_5$ compound. In **5** (Ln = Er), the distances of Ln−O and Ln⋯Ln are consistent with those in the similar nonanuclear Y$_9$ species^{15} as the radii of Y and Er are almost the same.

The Ln$_9$ core (Figure 1a) looks like an hourglass, and the whole anion (Figure 1b) is of somewhat solid wheel-shape with an underside diameter of 2.22 nm and a width of 1.56 nm. The middle of the "wheel" shrinks with a diameter of 1.67 nm. The planes of phenyl groups are ca. 38° and 42° inclined with respect to the square plane of four Ln1 for t-BA and μ-BA, respectively. There are six anions in each unit cell, and the packing arrangement of the anions leads to the formation of large hexagonal channels along the body diagonal directions (Figure 2). The channel changes its

(21) Bürgstein, M. R.; Roesky, P. W. *Angew. Chem., Int. Ed.* **2000**, *39*, 549.
(22) Lam, A. W. H.; Wong, W. T.; Wen, G. H.; Zhang, X. X.; Gao, S. *New J. Chem.* **2001**, *25*, 531.
(23) Boeyens, J. C. A.; Villiers, J. P. R. D. *J. Cryst. Mol. Struct.* **1972**, *2*, 197.
(24) Xiong, R. G.; Zuo, J. L.; Yu, Z.; You, X. Z.; Chen, W. *Inorg. Chem. Commun.* **1999**, *2*, 490.
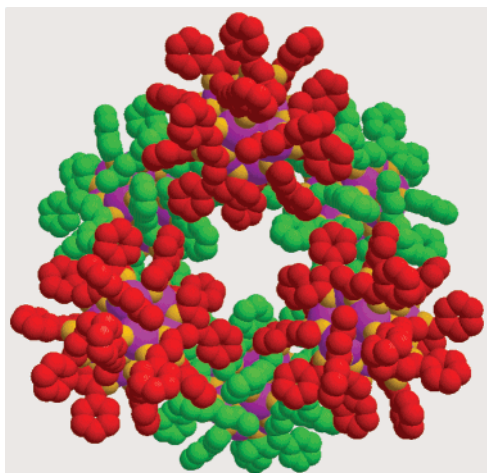
Figure 2. The packing of the nonanuclear anion (space-filling model) of **1** down the [111] direction, showing the hexagonal channel along the body diagonal direction in the lattice. Colors used: green and red for C, purple for Sm, and orange for O.

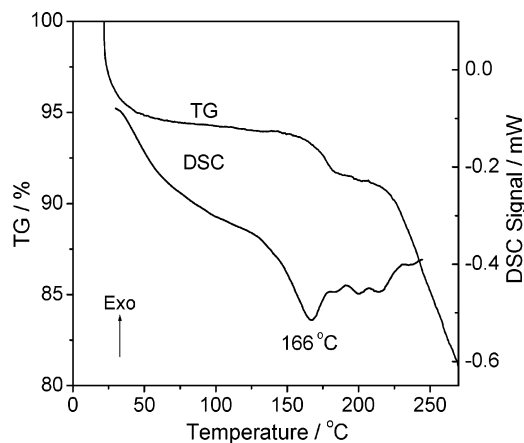**Figure 3.** Combined TG−DSC run of **1**.

Figure 4. Fluorescence spectrum ($\lambda_{ex} = 465$ nm) and excitation spectrum (inset) of **2**.

diameter (expanding and shrinking) in its running direction, and the minimum diameter is ca. 7 Å with van der Waals volume excluded. It is large enough for the solvent molecules and cations to move freely. In the lattice, the channels extend along the four body diagonal directions of the unit cell. This results in the severe disorder of the small components, which cannot be resolved by X-ray analysis even at 120 K, and in easy loss of the solvent for the crystals.

IR, FAB MS, and TG−DSC Characterizations. The IR spectra of the as-precipitated powder and the as-recrystallized crystal are identical, which implies the same purity of the two. A broad absorption appears at around 3350 cm^{-1}, the typical stretching of alcohol hydroxyl, indicating the presence of methanol. A weak peak around 3580 cm^{-1}, previously reported and assigned to the stretching of μ_3-OH,[25] was observed in these compounds and was probably obscured by the broad absorption of alcohol hydroxyl. Metal coordination results in appreciable shifts of the asymmetric stretching frequency of the diketone moiety of the BA ligand, from 1603, 1571 to about 1599, 1570, 1518 cm^{-1}, which happens to be coincident with those of the benzene moiety. A strong sharp absorption around 1380 cm^{-1} is assigned to the bending of CH$_3$ belonging to the methyl ketone.[26] The identity of the complexes was supported by the positive ion FAB MS study; a m/z value of 102 was observed for the [HN(CH$_2$-CH$_3$)$_3$]$^+$ counterion, which suggests the [Ln$_9$O$_2$(OH)$_8$(BA)$_{16}$] species is a monovalent anion. Although the crystals undergo rapid solvent loss once they leave the mother liquid, the compounds are stable according to thermal stability study. The TG trace of **1** (Figure 3) shows a weight loss of 5% before 50 °C, which corresponds to the loss of absorbed solvent (methanol and/or chloroform). No chemical decomposition is observed up to 150 °C. A weight loss of ca. 2.3% appears in the temperature range 150−190 °C, which indicates the loss of one [N(CH$_2$CH$_3$)$_3$] molecule per unit
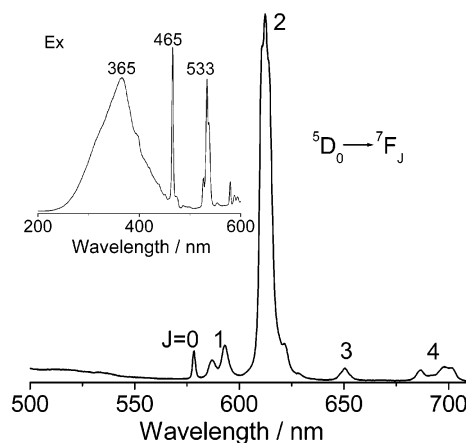
formula. Correspondingly, one endothermic peak appears in the DSC curve around 166 °C, with an enthalpy of approximate −50 kJ mol^{-1}. As the temperature exceeds 190 °C, the complex begins to decompose. Similar thermal behaviors are observed for **2**−**4**. Therefore, the nonanuclear species seem to be stable up to at least 150 °C.

Luminescence Spectroscopy of 2. The luminescence spectrum of the powder of complex **2** (Figure 4) at room temperature indicates that the cluster exhibits very strong red luminescence, which may arise from a $^5D_0 \rightarrow ^7F_J$ ($J = 0$−4) transition, a typical characteristic of Eu^{3+}.[27] The main emission occurs, as expected, in the $^5D_0 \rightarrow ^7F_2$. Although the $^5D_0 \rightarrow ^7F_0$ and $^5D_0 \rightarrow ^7F_1$ transitions are also present, they are 60 and 10 times less intense, respectively, which are in accordance with those observed in the Eu(btfa)$_3$·bipy.[28] The $^5D_0 \rightarrow ^7F_0$ transition is a singlet. The existence of a single peak at about 578 nm indicates the presence of only one single emitting species corresponding to the Eu1 of C_{2v} symmetry,[27] which is 8 times more than the Eu2 of D_{4d} symmetry in the nonanuclear cluster.

(25) Dubé, T.; Gambarotta, S.; Yap, G. *Organometallics* **1998**, *17*, 3967.
(26) *Infrared and Raman Spectra of Inorganic and Coordination Compounds*, 4th ed.; Nakamoto, K., Ed.; Wiley-Interscience: New York, 1986; p 260.

(27) (a) Vicentini, G.; Zinner, L. B.; Zukerman-Schpector, J.; Zinner, K. *Coord. Chem. Rev.* **2000**, *196*, 353. (b) Lessmann, J. J.; Horrocks, W. D. *Inorg. Chem.* **2000**, *39*, 3114.
(28) Batista, H. J.; de Andrade, A. V. M.; Longo, R. L.; Simas, A. M.; de Sá, G. F.; Ito, N. K.; Thompson, L. C. *Inorg. Chem.* **1998**, *37*, 3542.

Magnetic Properties. The temperature dependences of effective magnetic moment, μ_{eff}, of complexes **1**–**5** in the temperature range 2–300 K were studied. For complex **3** (Ln = Gd), the plot of χ_M^{-1} vs T obeys the Curie–Weiss law $[\chi = C/(T - \theta)]$ with Curie constant, χ, of 77.3 cm^3 K mol^{-1}, and with Weiss constant, θ, of -4.06. The μ_{eff} value per molecule of **3** is 23.6 μ_B at room temperature, close to the expected value of 23.8 μ_B for nine free noninteracting Gd^{3+} ions,[29] decreases gradually to 22.8 μ_B at 50 K, and then drops rapidly below 50 K to 15.2 μ_B at 2 K. The dramatic decrease of μ_{eff} at low temperature is mainly attributed to the weak intra- and intermolecular antiferromagnetic coupling between the Gd^{3+} ions[30] and may also partially arise from the very small splitting of the $^8S_{7/2}$ multiplet at zero field.[22] Similar varieties of the temperature dependence of μ_{eff} can also be found in complexes **4** and **5**. The decrease of μ_{eff} at low temperature is primarily due to the splitting of the ligand field of the Ln^{3+} ion because of strong spin–orbit coupling, and partly contributed to by the possible antiferromagnetic interaction between the Ln^{3+} ions. However, for complexes **1** and **2**, there is a continuous decrease in μ_{eff} as the temperature drops, which mainly indicates the feature of single Ln^{3+} ion.

[Ln$_5$(μ_4-O)(μ_3-OH)$_4$]$^{9+}$ Unit. It is interesting to compare the structure of nonanuclear clusters with other related complexes. The nonanuclear core contains two [Ln$_5$(μ_4-O)(μ_3-OH)$_4$]$^{9+}$ units and is constructed by sharing the apical lanthanide ion of the pentanuclear square-pyramidal units. Admittedly, the square-pyramidal core is extremely different from the cubane-like tetranuclear [Ln$_4$(μ_3-OH)$_4$]$^{8+}$ unit[18] and appears to be another common structural motif in lanthanide oxo–hydroxo clusters, as demonstrated by present work and others.[15,21,24] The hexanuclear octahedral oxo–hydroxo [Ln$_6$-(μ_6-O)(μ_3-OH)$_8$]$^{8+}$ cluster[14] may also be considered as two square-pyramidal units sharing their base. The reported pentanuclear [Eu$_5$(μ_4-OH)(μ_3-OH)$_4$(DBM)$_{10}$],[24] nonanuclear [Y$_9$(μ_4-O)$_2$(μ_3-OH)$_8$(AAA)$_{16}$],[15] and tetradecanuclear [Ln$_{14}$-(μ_4-OH)$_2$(μ_3-OH)$_{16}$(*o*-O$_2$NC$_6$H$_4$O)$_{24}$ (Ln = Er, Yb)][21] can all be regarded as being composed of one or more [Ln$_5$(μ_4-O)-(μ_3-OH)$_4$]$^{9+}$ units. The ligands utilized in these compounds as well as in this study are β-diketone or its analogue, which feature different coordination modes and seem to play an important role in the formation of the polynuclear lanthanide clusters. Moreover, the number of the square-pyramidal units in the cluster seems to have some relationship with the steric restriction of the ligand, i.e., the smaller ligand chosen, the larger complex gained. The novel example, the Ln$_{14}$(OH)$_{18}$ cluster,[21] can be described as a chain of two face-sharing square-antiprisms which contains four square-pyramidal units. From the discussion above, polynuclear lanthanide oxo–hydroxo clusters with designed nuclear number of $5n - 1$ ($n \geq 2$) can be probably deduced and obtained with specific ligands under appropriate reaction conditions.

Conclusion

A series of nonanuclear lanthanide oxo–hydroxo complexes with β-diketonate ligands have been assembled which contain two pentanuclear square-pyramidal units. The [Ln$_5$-(μ_4-O)(μ_3-OH)$_4$]$^{9+}$ core containing cluster may be a common structural motif in lanthanide polynuclear complexes as well as useful precursors for various advanced material processes. The structural integrity and the highly ordered arrangement of lanthanide centers in these nanosized clusters promise their applications as structural and functional building blocks for a variety of lanthanide-containing materials.

Supporting Information Available: Emission spectrum data ($\lambda_{\text{ex}} = 465$ nm) of the $^5D_0 \rightarrow {}^7F_J$ transitions in compound **2** and the temperature dependence of the effective magnetic moment of **1**–**5**. X-ray crystallographic data in CIF format for the five compounds in Table 1. This material is available free of charge via the Internet at http://pubs.acs.org.

IC025929U

(29) Kahn, O. *Molecular Magnetism*; VCH Publishers: New York, 1993.
(30) (a) Panagiotopoulos, A.; Zafiropoulos, T. F.; Perlepes, S. P.; Bakalbassis, E.; Massonramade, I.; Kahn, O.; Terzis, A.; Raptopoulou, C. P. *Inorg. Chem.* **1995**, *34*, 4918. (b) Costes, J. P.; Dahan, F.; Dupuis, A.; Lagrave, S.; Laurent, J. P. *Inorg. Chem.* **1998**, *37*, 153.